EUROPEAN ORGANIZATION FOR NUCLEAR RESEARCH

CERN-EP/2000-102
21 July 2000

Search for Single Top Production in e^+e^- Collisions at $\sqrt{s} = 189 - 202$ GeV

The ALEPH Collaboration[1]

Abstract

Single top production via flavour changing neutral currents in the reactions $e^+e^- \to \bar{t}c/u$ is searched for in approximately 411 pb^{-1} of data collected by ALEPH at centre-of-mass energies in the range between 189 and 202 GeV. In total, 58 events are selected in the data to be compared with 50.3 expected from Standard Model backgrounds. No deviation from the Standard Model expectation is observed. Upper limits at 95% CL on single top production cross sections at $\sqrt{s} = 189 - 202$ GeV are derived. A model-dependent limit on the sum of branching ratios $BR(t \to Zc) + BR(t \to Zu) < 17\%$ is obtained.

(To be submitted to Physics Letters B)

[1]See next pages for the list of authors.

The ALEPH Collaboration

R. Barate, D. Decamp, P. Ghez, C. Goy, S. Jezequel, J.-P. Lees, F. Martin, E. Merle, M.-N. Minard, B. Pietrzyk

Laboratoire de Physique des Particules (LAPP), IN^{2}P^3-CNRS, F-74019 Annecy-le-Vieux Cedex, France

R. Alemany, S. Bravo, M.P. Casado, M. Chmeissani, J.M. Crespo, E. Fernandez, M. Fernandez-Bosman, Ll. Garrido,[15] E. Graugés, A. Juste, M. Martinez, G. Merino, R. Miquel, Ll.M. Mir, P. Morawitz, A. Pacheco, I. Riu, H. Ruiz

Institut de Física d'Altes Energies, Universitat Autònoma de Barcelona, E-08193 Bellaterra (Barcelona), Spain[7]

A. Colaleo, D. Creanza, M. de Palma, G. Iaselli, G. Maggi, M. Maggi, S. Nuzzo, A. Ranieri, G. Raso, F. Ruggieri, G. Selvaggi, L. Silvestris, P. Tempesta, A. Tricomi,[3] G. Zito

Dipartimento di Fisica, INFN Sezione di Bari, I-70126 Bari, Italy

X. Huang, J. Lin, Q. Ouyang, T. Wang, Y. Xie, R. Xu, S. Xue, J. Zhang, L. Zhang, W. Zhao

Institute of High Energy Physics, Academia Sinica, Beijing, The People's Republic of China[8]

D. Abbaneo, G. Boix,[6] O. Buchmüller, M. Cattaneo, F. Cerutti, V. Ciulli, G. Davies, G. Dissertori, H. Drevermann, R.W. Forty, M. Frank, F. Gianotti, T.C. Greening, A.W. Halley, J.B. Hansen, J. Harvey, P. Janot, B. Jost, M. Kado, O. Leroy, P. Maley, P. Mato, A. Minten, A. Moutoussi, F. Ranjard, L. Rolandi, D. Schlatter, M. Schmitt,[20] O. Schneider,[2] P. Spagnolo, W. Tejessy, F. Teubert, E. Tournefier, A. Valassi, A.E. Wright

European Laboratory for Particle Physics (CERN), CH-1211 Geneva 23, Switzerland

Z. Ajaltouni, F. Badaud G. Chazelle, O. Deschamps, S. Dessagne, A. Falvard, C. Ferdi, P. Gay, C. Guicheney, P. Henrard, J. Jousset, B. Michel, S. Monteil, J-C. Montret, D. Pallin, J.M. Pascolo, P. Perret, F. Podlyski

Laboratoire de Physique Corpusculaire, Université Blaise Pascal, IN^{2}P^3-CNRS, Clermont-Ferrand, F-63177 Aubière, France

J.D. Hansen, J.R. Hansen, P.H. Hansen,[1] B.S. Nilsson, B. Rensch, A. Wäänänen

Niels Bohr Institute, 2100 Copenhagen, DK-Denmark[9]

G. Daskalakis, A. Kyriakis, C. Markou, E. Simopoulou, A. Vayaki

Nuclear Research Center Demokritos (NRCD), GR-15310 Attiki, Greece

A. Blondel, J.-C. Brient, F. Machefert, A. Rougé, M. Swynghedauw, R. Tanaka H. Videau

Laboratoire de Physique Nucléaire et des Hautes Energies, Ecole Polytechnique, IN^{2}P^3-CNRS, F-91128 Palaiseau Cedex, France

E. Focardi, G. Parrini, K. Zachariadou

Dipartimento di Fisica, Università di Firenze, INFN Sezione di Firenze, I-50125 Firenze, Italy

M. Corden, C. Georgiopoulos

Supercomputer Computations Research Institute, Florida State University, Tallahassee, FL 32306-4052, USA[13,14]

A. Antonelli, G. Bencivenni, G. Bologna,[4] F. Bossi, P. Campana, G. Capon, V. Chiarella, P. Laurelli, G. Mannocchi,[1,5] F. Murtas, G.P. Murtas, L. Passalacqua, M. Pepe-Altarelli

Laboratori Nazionali dell'INFN (LNF-INFN), I-00044 Frascati, Italy

M. Chalmers, J. Kennedy, J.G. Lynch, P. Negus, V. O'Shea, B. Raeven, D. Smith, P. Teixeira-Dias, A.S. Thompson, J.J. Ward

Department of Physics and Astronomy, University of Glasgow, Glasgow G12 8QQ,United Kingdom[10]

R. Cavanaugh, S. Dhamotharan, C. Geweniger,[1] P. Hanke, V. Hepp, E.E. Kluge, G. Leibenguth,

A. Putzer, K. Tittel, S. Werner,[19] M. Wunsch[19]

Kirchhoff-Institut für Physik, Universität Heidelberg, D-69120 Heidelberg, Germany[16]

R. Beuselinck, D.M. Binnie, W. Cameron, P.J. Dornan, M. Girone, S. Goodsir, N. Marinelli, E.B. Martin, J. Nash, J. Nowell, H. Przysiezniak,[1] A. Sciabà, J.K. Sedgbeer, J.C. Thompson,[24] E. Thomson, M.D. Williams

Department of Physics, Imperial College, London SW7 2BZ, United Kingdom[10]

V.M. Ghete, P. Girtler, E. Kneringer, D. Kuhn, G. Rudolph

Institut für Experimentalphysik, Universität Innsbruck, A-6020 Innsbruck, Austria[18]

C.K. Bowdery, P.G. Buck, G. Ellis, A.J. Finch, F. Foster, G. Hughes, R.W.L. Jones, N.A. Robertson, M. Smizanska, M.I. Williams

Department of Physics, University of Lancaster, Lancaster LA1 4YB, United Kingdom[10]

I. Giehl, F. Hölldorfer, K. Jakobs, K. Kleinknecht, M. Kröcker, A.-S. Müller, H.-A. Nürnberger, G. Quast, B. Renk, E. Rohne, H.-G. Sander, S. Schmeling, H. Wachsmuth C. Zeitnitz, T. Ziegler

Institut für Physik, Universität Mainz, D-55099 Mainz, Germany[16]

A. Bonissent, J. Carr, P. Coyle, A. Ealet, D. Fouchez, P. Payre, D. Rousseau, A. Tilquin

Centre de Physique des Particules, Faculté des Sciences de Luminy, IN^{2}P^3-CNRS, F-13288 Marseille, France

M. Aleppo, M. Antonelli, S. Gilardoni, F. Ragusa

Dipartimento di Fisica, Università di Milano e INFN Sezione di Milano, I-20133 Milano, Italy.

V. Büscher, H. Dietl, G. Ganis, K. Hüttmann, G. Lütjens, C. Mannert, W. Männer, H.-G. Moser, S. Schael, R. Settles, H. Seywerd, H. Stenzel, W. Wiedenmann, G. Wolf

Max-Planck-Institut für Physik, Werner-Heisenberg-Institut, D-80805 München, Germany[16]

P. Azzurri, J. Boucrot, O. Callot, S. Chen, M. Davier, L. Duflot, J.-F. Grivaz, Ph. Heusse, A. Jacholkowska,[1] J. Lefrançois, L. Serin, J.-J. Veillet, I. Videau,[1] J.-B. de Vivie de Régie, D. Zerwas

Laboratoire de l'Accélérateur Linéaire, Université de Paris-Sud, IN^{2}P^3-CNRS, F-91898 Orsay Cedex, France

G. Bagliesi, T. Boccali, C. Bozzi,[12] G. Calderini, R. Dell'Orso, I. Ferrante, A. Giassi, A. Gregorio, F. Ligabue, P.S. Marrocchesi, A. Messineo, F. Palla, G. Rizzo, G. Sanguinetti, G. Sguazzoni, R. Tenchini,[1] A. Venturi, P.G. Verdini

Dipartimento di Fisica dell'Università, INFN Sezione di Pisa, e Scuola Normale Superiore, I-56010 Pisa, Italy

G.A. Blair, J. Coles, G. Cowan, M.G. Green, D.E. Hutchcroft, L.T. Jones, T. Medcalf, J.A. Strong

Department of Physics, Royal Holloway & Bedford New College, University of London, Surrey TW20 OEX, United Kingdom[10]

D.R. Botterill, R.W. Clifft, T.R. Edgecock, P.R. Norton, I.R. Tomalin

Particle Physics Dept., Rutherford Appleton Laboratory, Chilton, Didcot, Oxon OX11 OQX, United Kingdom[10]

B. Bloch-Devaux, P. Colas, B. Fabbro, G. Faï̈f, E. Lançon, M.-C. Lemaire, E. Locci, P. Perez, J. Rander, J.-F. Renardy, A. Rosowsky, P. Seager,[23] A. Trabelsi,[21] B. Tuchming, B. Vallage

CEA, DAPNIA/Service de Physique des Particules, CE-Saclay, F-91191 Gif-sur-Yvette Cedex, France[17]

S.N. Black, J.H. Dann, C. Loomis, H.Y. Kim, N. Konstantinidis, A.M. Litke, M.A. McNeil, G. Taylor

Institute for Particle Physics, University of California at Santa Cruz, Santa Cruz, CA 95064, USA[22]

C.N. Booth, S. Cartwright, F. Combley, P.N. Hodgson, M. Lehto, L.F. Thompson

Department of Physics, University of Sheffield, Sheffield S3 7RH, United Kingdom[10]

K. Affholderbach, A. Böhrer, S. Brandt, C. Grupen, J. Hess, A. Misiejuk, G. Prange, U. Sieler
Fachbereich Physik, Universität Siegen, D-57068 Siegen, Germany[16]

C. Borean, G. Giannini, B. Gobbo
Dipartimento di Fisica, Università di Trieste e INFN Sezione di Trieste, I-34127 Trieste, Italy

J. Putz, J. Rothberg, S. Wasserbaech, R.W. Williams
Experimental Elementary Particle Physics, University of Washington, WA 98195 Seattle, U.S.A.

S.R. Armstrong, P. Elmer, D.P.S. Ferguson, Y. Gao, S. González, O.J. Hayes, H. Hu, S. Jin, J. Kile, P.A. McNamara III, J. Nielsen, W. Orejudos, Y.B. Pan, Y. Saadi, I.J. Scott, J. Walsh, J.H. von Wimmersperg-Toeller, Sau Lan Wu, X. Wu, G. Zobernig
Department of Physics, University of Wisconsin, Madison, WI 53706, USA[11]

[1]Also at CERN, 1211 Geneva 23, Switzerland.
[2]Now at Université de Lausanne, 1015 Lausanne, Switzerland.
[3]Also at Centro Siciliano di Fisica Nucleare e Struttura della Materia, INFN Sezione di Catania, 95129 Catania, Italy.
[4]Also Istituto di Fisica Generale, Università di Torino, 10125 Torino, Italy.
[5]Also Istituto di Cosmo-Geofisica del C.N.R., Torino, Italy.
[6]Supported by the Commission of the European Communities, contract ERBFMBICT982894.
[7]Supported by CICYT, Spain.
[8]Supported by the National Science Foundation of China.
[9]Supported by the Danish Natural Science Research Council.
[10]Supported by the UK Particle Physics and Astronomy Research Council.
[11]Supported by the US Department of Energy, grant DE-FG0295-ER40896.
[12]Now at INFN Sezione di Ferrara, 44100 Ferrara, Italy.
[13]Supported by the US Department of Energy, contract DE-FG05-92ER40742.
[14]Supported by the US Department of Energy, contract DE-FC05-85ER250000.
[15]Permanent address: Universitat de Barcelona, 08208 Barcelona, Spain.
[16]Supported by the Bundesministerium für Bildung, Wissenschaft, Forschung und Technologie, Germany.
[17]Supported by the Direction des Sciences de la Matière, C.E.A.
[18]Supported by the Austrian Ministry for Science and Transport.
[19]Now at SAP AG, 69185 Walldorf, Germany
[20]Now at Harvard University, Cambridge, MA 02138, U.S.A.
[21]Now at Département de Physique, Faculté des Sciences de Tunis, 1060 Le Belvédère, Tunisia.
[22]Supported by the US Department of Energy, grant DE-FG03-92ER40689.
[23]Supported by the Commission of the European Communities, contract ERBFMBICT982874.
[24]Also at Rutherford Appleton Laboratory, Chilton, Didcot, UK.

1 Introduction

The top quark is the heaviest known elementary particle: its mass has been measured at the Tevatron Collider to be $m_{\mathrm{t}} = 174.3 \pm 5.1\,\mathrm{GeV}/c^2$ [1]. At LEP2 single top production could be possible via flavour changing neutral currents (FCNC) in the reactions[1]

$$\mathrm{e^+e^-} \rightarrow \bar{\mathrm{t}}\mathrm{c/u}\,. \tag{1}$$

In the Standard Model (SM) such processes are forbidden at tree level and can only proceed via loops with cross sections $\lesssim 10^{-9}$ fb [2]. In addition a single top can be produced in the SM via the reaction $\mathrm{e^+e^-} \rightarrow \mathrm{e^-}\bar{\nu}_{\mathrm{e}}\mathrm{t}\bar{\mathrm{b}}$, also characterised by a very small cross section (of order 10^{-4} fb [3]). In this letter a search for single top production via the reaction $\mathrm{e^+e^-} \rightarrow \bar{\mathrm{t}}\mathrm{c/u}$ is reported. This search is based on all data collected by ALEPH at centre-of-mass energies between 189 and 202 GeV, corresponding to a total integrated luminosity of 411 pb^{-1}.

Extensions of the Standard Model could in fact lead to enhancements of FCNC single top production and to measurable effects as proposed, for example, in Refs. [4–12]. Upper limits (at 95% CL) on FCNC in the top sector have been derived by CDF from a search for the decays $\mathrm{t} \rightarrow \gamma\mathrm{c/u}$ and $\mathrm{t} \rightarrow \mathrm{Zc/u}$ [13]:

$$\mathrm{BR}(\mathrm{t} \rightarrow \gamma\mathrm{c}) + \mathrm{BR}(\mathrm{t} \rightarrow \gamma\mathrm{u}) \;<\; 3.2\% \tag{2}$$

$$\mathrm{BR}(\mathrm{t} \rightarrow \mathrm{Zc}) + \mathrm{BR}(\mathrm{t} \rightarrow \mathrm{Zu}) \;<\; 33\%\,. \tag{3}$$

It is customary to parametrise the FCNC transitions in terms of anomalous vertices whose strengths are described by two parameters k_{Z} and k_γ for Z and γ exchange, respectively. Using the formalism of Ref. [12], the vertices for the transitions $\gamma \rightarrow \mathrm{f}\bar{\mathrm{f}}'$ and $\mathrm{Z} \rightarrow \mathrm{f}\bar{\mathrm{f}}'$ are assumed to have the following form [8]:

$$\Gamma^{\gamma}_{\mu} \;=\; k_\gamma \frac{e e_{\mathrm{q}}}{\Lambda} \sigma_{\mu\nu} q^{\nu} \tag{4}$$

$$\Gamma^{\mathrm{Z}}_{\mu} \;=\; k_{\mathrm{Z}} \frac{e}{\sin 2\theta_{\mathrm{W}}} \gamma_{\mu}\,. \tag{5}$$

Here, Λ is the new physics cutoff, e is the electron charge, e_{q} the top quark charge, θ_{W} is the weak mixing angle and $\sigma^{\mu\nu} = \frac{1}{2}(\gamma^\mu\gamma^\nu - \gamma^\nu\gamma^\mu)$. In the following it is assumed that k_γ and k_{Z} are real and positive and that $\Lambda = m_{\mathrm{t}}$.

From the CDF experimental limits (Eqns. 2 and 3) and the definitions in Eqns. 4 and 5, the following 95% CL upper limits on the anomalous couplings are derived:

$$k_\gamma^2 \;<\; 0.176 \tag{6}$$

$$k_{\mathrm{Z}}^2 \;<\; 0.533\,. \tag{7}$$

The cross section for $\bar{\mathrm{t}}\mathrm{c/u}$ production in $\mathrm{e^+e^-}$ collisions is given at the Born level by the following expression:

$$\sigma(\mathrm{e^+e^-} \rightarrow \bar{\mathrm{t}}\mathrm{c}) = \frac{\pi\alpha^2}{s}\left(1 - \frac{m_{\mathrm{t}}^2}{s}\right)^2 \left[k_\gamma^2 e_{\mathrm{q}}^2 \frac{s}{m_{\mathrm{t}}^2}\left(1 + 2\frac{m_{\mathrm{t}}^2}{s}\right) + \right.$$
$$\left. + \frac{k_{\mathrm{Z}}^2 (1 + {a_{\mathrm{W}}}^2)(2 + m_{\mathrm{t}}^2/s)}{4\sin^4 2\theta_{\mathrm{W}}(1 - m_{\mathrm{Z}}^2/s)^2} + 3 k_\gamma k_{\mathrm{Z}} \frac{a_{\mathrm{W}} e_{\mathrm{q}}}{\sin^2 2\theta_{\mathrm{W}}(1 - m_{\mathrm{Z}}^2/s)}\right]\,, \tag{8}$$

[1] Throughout this paper, the notation $\bar{\mathrm{t}}\mathrm{c}$ is used for both $\bar{\mathrm{t}}\mathrm{c}$ and $\bar{\mathrm{c}}\mathrm{t}$.

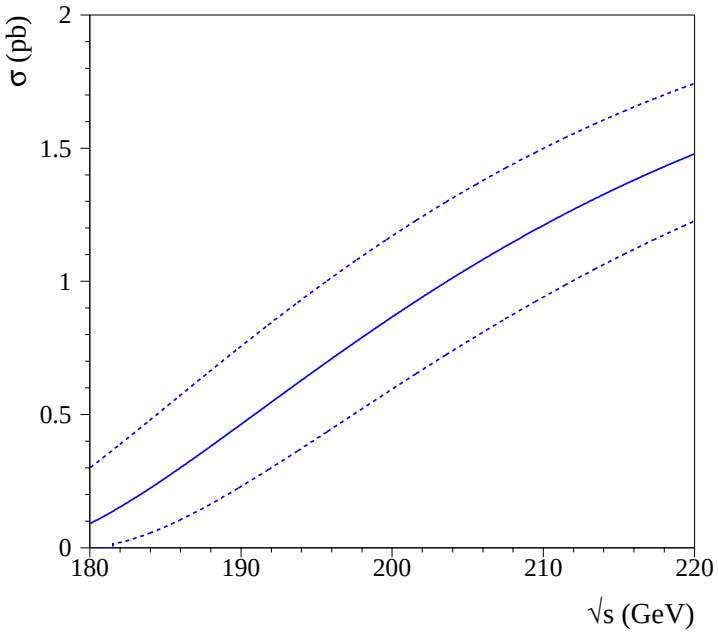

Figure 1: Cross section for $\bar{\mathrm{t}}\mathrm{c}/\mathrm{u}$ production as a function of centre-of-mass energy with coupling constants fixed to the CDF limits. The solid curve corresponds to a top mass of 174 GeV/c^2. The upper (lower) dashed curve corresponds to a top mass of 169 (179) GeV/c^2.

where α is the fine structure constant, s is the centre-of-mass energy squared, m_{Z} is the Z mass and $a_{\mathrm{W}} = 1 - 4\sin^2\theta_{\mathrm{W}}$. The three terms appearing in Eq. 8 describe γ exchange, Z exchange and γ-Z interference, respectively. Corrections related to the nonzero widths of t quark and W boson are entirely negligible at the LEP2 centre-of-mass energies [8]. Figure 1 shows the cross section as a function of $\sqrt{s}$ evaluated with $m_{\mathrm{t}} = 174 \pm 5$ GeV/c^2 and with the inclusion of QCD corrections [14]. The coupling constants k_γ and k_{Z} have been fixed to the CDF upper limits. With this choice of parameters, the contribution to the cross section associated to the γ exchange term is very small at these centre-of-mass energies.

The CDF limits constrain only weakly the FCNC branching ratios (Eqns. 2,3), so that BR($\mathrm{t} \to \mathrm{bW}$) could be as small as 64%. In this analysis, only the $\mathrm{t} \to \mathrm{bW}$ decay is searched for and results are given in terms of $\sigma\,(\mathrm{e^+e^-} \to \bar{\mathrm{t}}\mathrm{c}/\mathrm{u}) \times \mathrm{BR}(\mathrm{t} \to \mathrm{bW})$. When limits on the k_{Z} and k_γ couplings are derived, the reduction of BR($\mathrm{t} \to \mathrm{bW}$) due to possible FCNC decays of the top is taken into account.

2 The ALEPH detector

A detailed description of the ALEPH detector is presented in Ref. [15], and an account of its performance as well as a description of the standard analysis algorithms can be found in Ref. [16]. Only a brief overview is given here.

The tracking system consists of a silicon vertex detector, a drift chamber and a large time projection chamber, immersed in a 1.5 T axial magnetic field produced

by a superconducting magnet. The silicon vertex detector (VDET) provides precise track measurements close to the interaction point. It consists of two concentric layers of double-sided silicon microstrip detectors positioned at average radii of 6.5 cm and 11.3 cm, covering 95% and 88% of the solid angle, respectively. The vertex detector is surrounded by a multi-layer axial-wire cylindrical drift chamber, the inner tracking chamber (ITC), which is 200 cm long and measures the $r\phi$ positions of tracks at 8 radii between 16 and 26 cm. The time projection chamber (TPC) is the main tracking detector. It is 440 cm long and provides up to 21 three-dimensional space coordinates and 338 samples of ionization energy loss (dE/dx) at radii between 30 and 180 cm. Using the combined information from the TPC, ITC and VDET, a transverse momentum resolution of $\sigma(1/p_{\mathrm{t}}) = 0.6 \times 10^{-3}(\mathrm{GeV}/c)^{-1} \oplus 0.005/p_{\mathrm{t}}$ is achieved.

The electromagnetic calorimeter, ECAL, is a lead/proportional wire chamber sampling device of 22 radiation length thickness which surrounds the TPC and is contained inside the superconducting coil. Its relative energy resolution is $\sigma(E)/E = 0.18/\sqrt{E} + 0.009$ with E in GeV.

The return yoke of the magnetic field is a large iron structure fully instrumented to form a hadron calorimeter, HCAL, which also serves as a muon filter. The HCAL consists of 23 layers of streamer tubes 9×9 mm^2 in cross section separated by 5 cm thick iron slabs, giving a total of 7.2 interaction lengths. The relative energy resolution of the calorimeter is $\sigma(E)/E = 0.85/\sqrt{E}$ with E in GeV. Outside the iron structure, two double layers of streamer tubes, the muon chambers, provide two space coordinates for particles leaving the detector, thus improving the performance for muon identification.

The luminosity monitors (LCAL and SICAL) extend the calorimetric coverage down to polar angles of 34 mrad.

Using the energy flow algorithm described in [16], the measurements of the tracking detectors and calorimeters are combined into "objects" classified as electrons, muons, photons, and charged and neutral hadrons. A "good track" is defined as a charged particle track originating from within a cylinder of 2 cm radius and 20 cm length centred at the interaction point and parallel to the beam axis, having a polar angle $|\cos\theta| < 0.95$, and with at least four reconstructed coordinates in the TPC.

3 Monte Carlo simulation

All selection criteria were established on the basis of Monte Carlo simulation of signal and background events. The position of the most important cuts was determined following the $\bar{N}_{95}$ prescription [17], which corresponds to the minimisation of the expected 95% CL cross section upper limit in the absence of a signal.

To model the production of $\bar{\mathrm{t}}\mathrm{c}/\mathrm{u}$ in $\mathrm{e}^+\mathrm{e}^-$ collisions, a modified version of JETSET [18] was employed in which the top is produced together with a light quark and is forced to decay into bW. Because the top decays faster than the characteristic hadronization time, no top hadrons are formed. The b and c/u quarks are joined by a string to form a colour singlet. The b is allowed to develop a parton shower to take into account hard gluon emission and the recoil of gluon emission off the b is shared by the W [19]. Initial state radiation is implemented in the generator [20].

A sample of 2000 fully simulated events was produced for each of the two final states $\bar{\mathrm{t}}\mathrm{c}$ and $\bar{\mathrm{t}}\mathrm{u}$ at the different centre-of-mass energies of 189, 192, 196, 200 and 202 GeV and for three values of the top mass (169, 174 and 179 GeV/c^2).

For background studies, $q\overline{q}$ and four-fermion (WW, Weν, Zee and ZZ) event samples corresponding to integrated luminosities at least ten times that of the data were generated. For the $q\overline{q}$ simulation, both Monte Carlo generators PYTHIA [18] and KORALZ [21] were used. The KORALW [22] generator was used to produce WW events, while the simulation of other four-fermion final states was based on PYTHIA.

4 Analysis

At the LEP2 centre-of-mass energies the top would be produced very close to threshold. This leads to characteristic kinematic properties of the final state. When the top is produced at rest ($E_{\mathrm{t}} \simeq m_{\mathrm{t}}$), the light quark accompanying the top has a small energy ($E_{\mathrm{c/u}} \simeq \sqrt{s} - m_{\mathrm{t}}$) and the b and W from the top decay are almost monochromatic, with energies given by the following expressions:

$$E_{\mathrm{b}} \simeq \frac{m_{\mathrm{t}}^2 - m_{\mathrm{W}}^2 + m_{\mathrm{b}}^2}{2m_{\mathrm{t}}}, \tag{9}$$

$$E_{\mathrm{W}} \simeq \frac{m_{\mathrm{t}}^2 + m_{\mathrm{W}}^2 - m_{\mathrm{b}}^2}{2m_{\mathrm{t}}}. \tag{10}$$

In this analysis no attempt is made to identify the light quark flavour. In the following, every reference to c quarks also applies to u quarks.

A loose preselection is first applied. The preselection is followed by two separate analyses, designed for the two possible decays of the W, leptonic and hadronic. The leptonic W decay analysis is applied if at least one isolated electron or muon is found; in this case the rest of the event is forced into two jets. If no isolated lepton is found the event is forced into four jets and the hadronic W decay analysis is applied.

To tag the b jet, the confidence level CL that all the charged tracks of a jet originate from the primary vertex is computed [23]. The jets are ordered by decreasing $-\log(\mathrm{CL})$ (denoted as "b tag"), and the one with the largest b tag is identified as the b jet. In some cases, however, the c jet can have a higher b tag than the b jet. To correct for this wrong assignment the kinematic properties of the signal decay are used: when the energy of the jet with the highest b tag is smaller than 30 GeV, the one with the second highest b tag probability is taken as the b jet. In the events classified as four jets the c jet is identified as the least energetic one.

The preselection is based on the following cuts. To reject dilepton events at least nine good tracks must be reconstructed in the event. To reject $\gamma\gamma$ interactions, the total event energy and invariant mass are required to be larger than 100 GeV and 50 GeV/c^2, respectively. The total longitudinal momentum of the event must be smaller than 55 GeV and no photon with energy larger than 38 GeV must be reconstructed; these cuts mainly reject radiative returns to the Z. Moreover the charged multiplicity of each reconstructed jet is required to be larger than zero, to eliminate residual contamination from radiative Z returns.

According to the Monte Carlo simulation, the background surviving this preselection is composed of $q\overline{q}(\gamma)$ events (61%), WW events (35%) and other four-fermion processes (4%). After preselection 15249 events are selected in the data, to be compared with an expectation of 15268 events from Standard Model processes.

Table 1: Cuts used in the W leptonic and in the W hadronic decay selections. The variables are defined in the text.

W leptonic	W hadronic
$70 < m_{\ell\nu}\,(\mathrm{GeV}/c^2) < 90$	$0.57 < P_{\mathrm{qq}}/E_{\mathrm{qq}} < 0.73$
$m_{\mathrm{qq}}\,(\mathrm{GeV}/c^2) < 70$	$72 < m_{\mathrm{qq}}\,(\mathrm{GeV}/c^2) < 91$
$160 < m_{\mathrm{t}}\,(\mathrm{GeV}/c^2) < 187$	$55 < E(\mathrm{b\ jet})\,(\mathrm{GeV}) < 80$
$E(\mathrm{b\ jet})_{\mathrm{tcm}}$ (GeV)> 55	Thrust < 0.90
b tag > 2	$E_{\mathrm{tot}}\,(\mathrm{GeV}) > 145$
-	Highest jet b tag > 5.8
-	2nd highest jet b tag < 6

4.1 The leptonic W decay analysis

When the W decays leptonically the signal topology is characterised by an isolated, energetic lepton accompanied by two jets (the b and the c jets). An electron or muon is selected by applying the lepton identification described in [16]; the lepton is required to be energetic ($E_{\mathrm{lep}} > 10$ GeV) and isolated. The additional energy E_{iso} contained in a 30° cone around the lepton has to be less than 0.1 E_{lep}. For the identified electrons, photons are excluded from the computation of E_{iso}. No attempt to identify W decays into $\tau\ \nu$ is made here.

The lepton is removed and the rest of the event is forced into two jets with the JADE algorithm. By imposing energy-momentum conservation, the neutrino momentum is reconstructed as the missing momentum and the jet energies are recomputed (one-constraint fit). The velocity of the jets is kept fixed while the energies and the momenta are rescaled taking into account their experimental errors. With these rescaled quantities, two fitted masses $m_{\ell\nu}$ and m_{qq} are calculated.

The complete list of cuts is given in Table 1. The top mass m_{t} is calculated from the momenta of the neutrino, lepton, and b jet. For both the signal and the WW background, the variable $m_{\ell\nu}$ gives the W mass, while m_{qq} peaks at m_{W} only for WW events and assumes lower values for the signal where it provides the mass of the bc system. The variable $E(\mathrm{b\ jet})_{\mathrm{tcm}}$ is the b jet reconstructed energy evaluated in the top centre-of-mass frame, taking the top momentum to be opposite to that of the charm jet. Distributions of the most relevant variables used in this selection are shown in Fig. 2 for both signal and background.

The results of the selection are given in Table 2. The background is dominated by WW semileptonic decays. The signal efficiencies are independent of the flavour of the light quark (c or u) produced with the top and of whether the W decays to an electron or a muon.

4.2 The hadronic W decay analysis

If no isolated lepton is found the event is forced into four jets. The jet energies and momenta are rescaled by applying a four-constraint fit. The b and c jets are identified as described before and the two remaining jets are used to evaluate the W mass m_{qq} and momentum P_{qq}.

The complete list of cuts is given in Table 1. The "anti-b" cut for the jet with the second highest b tag probability reduces the background from $\mathrm{b\bar{b}}$ events. Contrary to

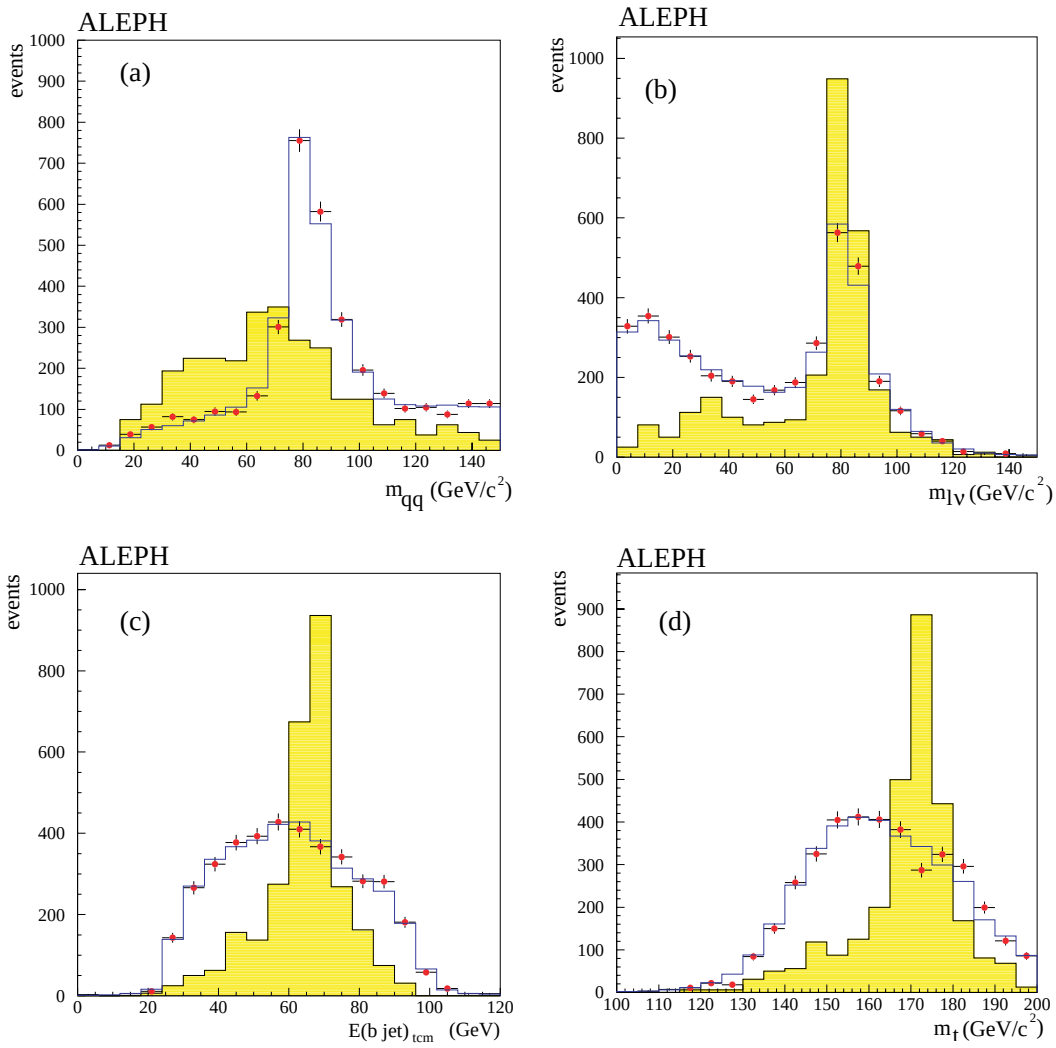

Figure 2: Distributions for leptonic W decays of signal (shaded histogram with arbitrary normalization), background (open histogram), and data from 189 to 202 GeV for the variables (a) m_{qq}, (b) $m_{\ell\nu}$, (c) $E(\mathrm{b\ jet})_{\mathrm{tcm}}$ and (d) m_{t}, after preselection.

the leptonic case, the b jet energy is here evaluated in the laboratory frame because the c jet direction is less well reconstructed. Distributions of the most relevant variables used in this selection are shown in Fig. 3 for both signal and background.

The results of the selection are given in Table 2. The background is approximately composed of 60% $\mathrm{q\overline{q}}$, 20% WW and 10% of other four-fermion events. The $\mathrm{q\overline{q}}$ background is dominated by the $\mathrm{b\bar{b}}$ component (85%) with an additional 12% of $\mathrm{c\bar{c}}$ and 3% of light quarks.

5 Results and systematic uncertainties

The analysis was applied to the data collected at centre-of-mass energies between 189 and 202 GeV during the 1998–1999 data-taking. A detailed breakdown of the luminosities at the different centre-of-mass energies is reported in Table 2.

In total six candidates are selected by the leptonic selection (5.7 expected) and 52 by the hadronic one (44.5 expected). No deviation from the Standard Model is

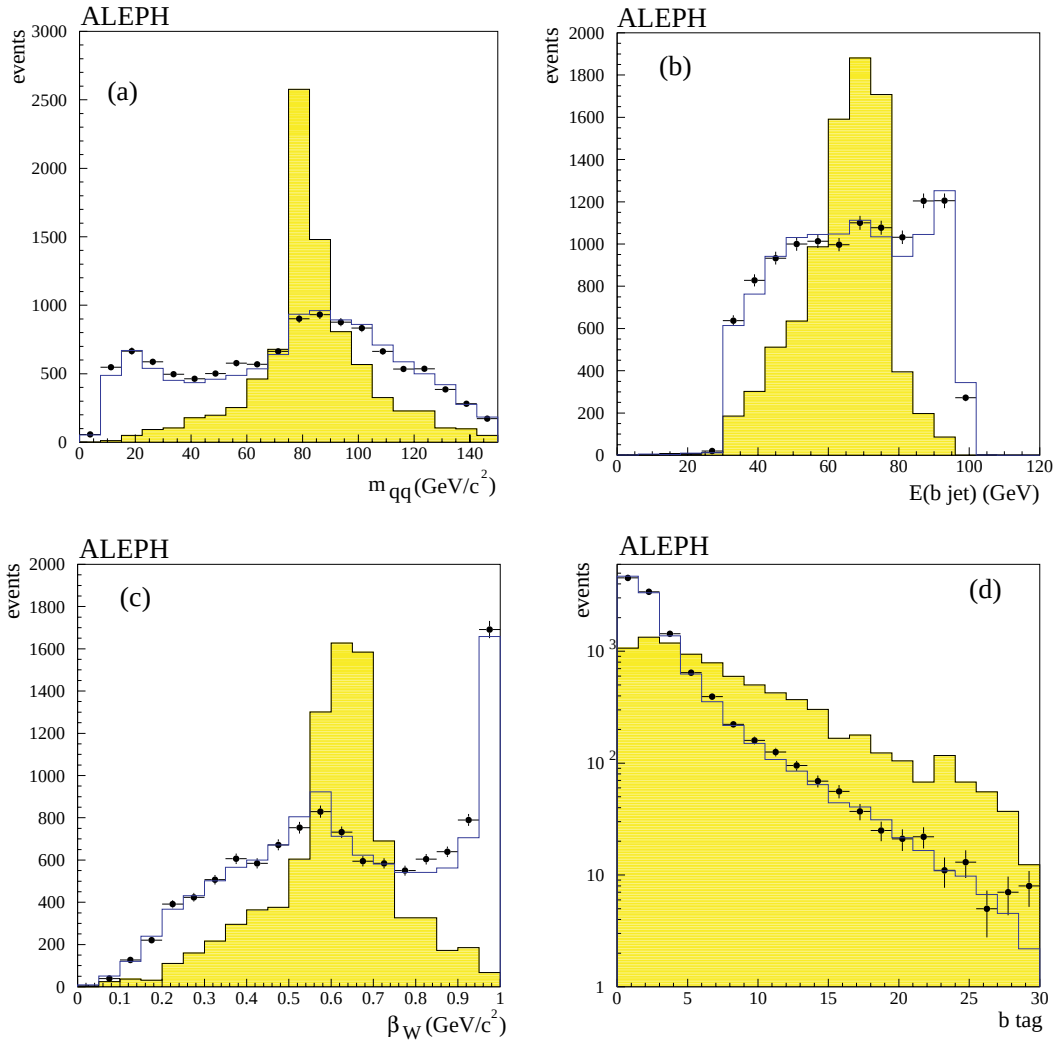

Figure 3: Distributions for hadronic W decays of signal (shaded histogram with arbitrary normalization), background (open histogram), and data from 189 to 202 GeV for the variables (a) m_{qq}, (b) E(b jet), (c) $\beta_{\mathrm{W}} = P_{\mathrm{qq}}/E_{\mathrm{qq}}$ and (d) b tag, after preselection.

observed. From these results limits on single top production and couplings are derived after subtraction of the expected background.

To assess the systematic uncertainty associated with the background estimate, the efficiencies in data and Monte Carlo were compared by applying one cut at a time after preselection. This study was performed with all data combined after having verified the consistency of the results for each energy point separately. The relative systematic uncertainties obtained with this procedure are summarised in Table 3. The differences between data and Monte Carlo for the individual variables are compatible with zero within the statistical uncertainty of the test, except for the b tag.

The expected background has therefore been corrected for the observed difference in the b tag efficiency for both the hadronic and leptonic channels. When extracting the limits, a systematic uncertainty equal to the quadratic sum of the statistical errors for the individual variables has been included by reducing the expected background by 6.2% and 2.8% for the leptonic and hadronic selections, respectively.

The systematic error associated with the jet energy calibration was evaluated by

Table 2: Performance and results of the analysis. At each centre-of-mass energy the number of expected background events ($N^{\rm bkg}$), of observed candidates ($N^{\rm obs}$), the signal efficiency ε computed with respect to all W decays, and the expected and measured 95% CL upper limits on single top production cross section ($\sigma_{95}^{\rm exp}$ and $\sigma_{95}^{\rm meas}$) are reported for both the leptonic and hadronic W decays; systematic uncertainties are not included in these cross section upper limits. A top mass of 174 GeV/c^2 is assumed. In the last row the measured 95% CL upper limits on single top production ($\sigma_{95}^{\rm meas-comb}$) obtained by combining the leptonic and hadronic channels and including the systematic uncertainties on background and on the signal efficiencies are given.

$\sqrt{s}$ (GeV)	188.6		191.6		195.5		199.5		201.6	
$\mathcal{L}$ (pb^{-1})	174		29		80		86		42	
	lept.	hadr.	lept.	hadr.	lept.	hadr.	lept.	hadr.	lept.	hadr.
$N_{\rm WW}^{\rm bkg}$	2.1	4.5	0.3	0.7	1.3	3.9	0.9	5.8	0.7	2.6
$N_{\rm 4f}^{\rm bkg}$	0.05	1.2	0.01	0.2	0.04	0.8	0.08	0.8	0.03	0.4
$N_{\rm qq}^{\rm bkg}$	0.09	10.6	0.02	1.8	0.06	5.5	0.06	3.7	0.06	2.0
$N_{\rm tot}^{\rm bkg}$	2.2	16.3	0.3	2.7	1.4	10.2	1.0	10.3	0.8	5.0
$N^{\rm obs}$	4	21	0	5	1	13	1	9	0	4
ε (%)	7.0	17	6.2	16	5.5	14.6	4.9	13.1	3.5	14.3
$\sigma_{95}^{\rm exp}$ (pb)	0.41	0.34	2.10	1.20	1.03	0.73	0.98	0.75	2.7	1.09
$\sigma_{95}^{\rm meas}$ (pb)	0.59	0.49	1.70	1.70	0.92	0.95	0.98	0.66	2.0	0.94
$\sigma_{95}^{\rm meas-comb}$ (pb)	0.33		1.18		0.67		0.48		0.72	

varying the jet energy corrections taken from [24] by one standard deviation. The change on the expected background is found to be negligible.

Concerning the signal, a large variation of the efficiency arises from the uncertainty on the top mass. A reduction of the efficiency of the order of 15% is obtained when the selection, optimized for $m_{\rm t} = 174$ GeV/c^2, is applied to signal events generated at $m_{\rm t} = 169$ and 179 GeV/c^2.

Other systematic uncertainties on the signal efficiency are related to the modelling of single top production and decay, and to the detector simulation. The impact of the modelling of the signal on the efficiency has been studied by varying model parameters such as the top production angle; negligible effects have been found. For what concerns detector effects the main source of systematic uncertainties is again related to the b tag efficiency. From studies based on events collected at the Z peak in 1998 and 1999, a total systematic uncertainty on the signal efficiency of 5% has been derived [25]. This uncertainty is conservatively applied as a net reduction of the signal efficiency when deriving the limits.

The results of this search are translated into cross section upper limits for single top production, as shown in Table 2. A 95% CL upper limit of 0.48 pb on the single top production cross section at $\sqrt{s} = 200\,\text{GeV}$ is obtained. This limit assumes a 100% branching ratio of top into bW and $m_{\rm t} = 174$ GeV/c^2. For a top mass of $m_{\rm t} = 169$ (179) GeV/c^2 the limit deteriorates to 0.53 (0.55) pb.

The likelihood ratio method is used for combining the results at the different energies to constrain the two couplings $k_{\rm Z}$ and k_γ. This combination is based on

Table 3: Relative systematic uncertainties on the background efficiency for each selection variable, determined by applying one cut at a time in data and Monte Carlo.

Leptonic W		Hadronic W	
Variable	$\frac{\varepsilon_{\rm data}-\varepsilon_{\rm MC}}{\varepsilon_{\rm MC}}$ (%)	Variable	$\frac{\varepsilon_{\rm data}-\varepsilon_{\rm MC}}{\varepsilon_{\rm MC}}$ (%)
Lepton ID	3.8 ± 3.3	$P_{\rm qq}/E_{\rm qq}$	1.2 ± 1.7
$m_{\rm qq}$	0.9 ± 3.6	$m_{\rm qq}$	-1.6 ± 1.6
$E(\text{b jet})_{\rm tcm}$	0.7 ± 1.3	$E(\text{b jet})$	0.4 ± 1.0
$m_{\ell\nu}$	2.5 ± 2.4	Thrust	0.2 ± 0.8
$m_{\rm t}$	0.3 ± 1.7	$E_{\rm tot}$	-0.3 ± 0.4
Highest jet b tag	5.1 ± 2.1	Highest jet b tag	9.6 ± 0.8

Eq. 8 with the inclusion of QCD corrections. Figure 4 shows the region of the $k_{\rm Z}$-k_γ plane excluded at 95% CL for different choices of the top mass. The exclusion curves include the reduction in BR(t $\to$ bW), computed as a function of $k_{\rm Z}$ and k_γ, due to possible FCNC decays of the top. The limits obtained by CDF are also shown. For $m_{\rm t} = 174$ and 169 GeV/c^2 the present analysis improves the CDF limit on $k_{\rm Z}$ while for $m_{\rm t} = 179$ GeV/c^2 only a slight improvement is obtained due to the lower single top production cross section.

A 95% CL upper limit of 0.53 for the anomalous coupling $k_{\rm Z}$ is obtained for $m_{\rm t} = 174$ GeV/c^2 and $k_\gamma = 0$. This exclusion translates into the branching ratio limit BR(t $\to$ Zc) + BR(t $\to$ Zu) $< 17\%$.

6 Conclusions

Single top production via flavour changing neutral currents has been searched for in 411 pb^{-1} of data collected by ALEPH at centre-of-mass energies in the range between 189 and 202 GeV. In total, 58 events were selected in the data to be compared with 50.2 expected from Standard Model backgrounds. Upper limits at 95% CL on single top production cross sections at $\sqrt{s} = 189 - 202$ GeV have been derived, for example 0.48 pb at $\sqrt{s} = 200\,$GeV. This assumes a 100% branching ratio of top into bW and $m_{\rm t} = 174$ GeV/c^2.

The combination of all data leads to a 95% CL model-dependent upper limit of 0.53 for $k_{\rm Z}$, the flavour changing coupling to the Z. This result is valid for $m_{\rm t} = 174$ GeV/c^2 and $k_\gamma = 0$. With the same assumptions a 95% CL upper limit of 17% on BR(t $\to$ Zc) + BR(t $\to$ Zu) is obtained, which improves on the previous CDF result.

Acknowledgements

We thank our colleagues from the CERN accelerator divisions for the successful operation of LEP. We are indebted to the engineers and technicians in all our institutions for their contribution to the continuing good performance of ALEPH. Those of us from non-member states thank CERN for its hospitality.

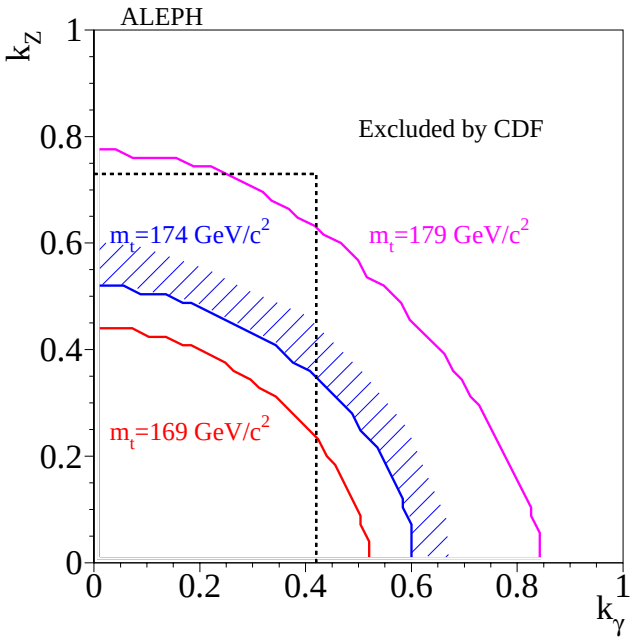

Figure 4: Exclusion curves at 95% CL in the k_Z-k_γ plane for three different values of m_t. The CDF exclusion [13] is also shown.

References

[1] CDF Collaboration, *Measurement of the top quark mass*, Phys. Rev. Lett. **80** (1998) 2767;
DØ Collaboration, *Direct measurement of the top quark mass at D0*, Phys. Rev. **D58** (1998) 052001.
For the combination of results, see, for example G. Brooijmans, Talk given at the 14th Rencontres de Physique de la Vallee d'Aoste, Feb. 2000, hep-ex/0005030.

[2] C.-S. Huang, X.-H. Wu and S.-H. Zhu, Phys. Lett. **B 452** (1999) 143.

[3] K. Hagiwara, M. Tanaka and T. Stelzer, Phys. Lett. **B 325** (1994) 521;
E. Boos *et al.*, Phys. Lett. **B 326** (1994) 190.

[4] B.A. Arbuzov and M.Y. Osipov, Phys. Atom. Nucl. **62** (1999) 485; Yad. Fiz. **62** (1999) 528.

[5] T. Han and J.L. Hewett, Phys. Rev. **D 60** (1999) 074015.

[6] H. Fritzsch and D.Holtmannspötter, Phys. Lett. **B 457** (1999) 186.

[7] S. Bar-Shalom and J. Wudka, Phys. Rev. **D 60** (1999) 094016.

[8] V.F. Obraztsov, S.R. Slabospitsky and O.P. Yushchenko, Phys. Lett. **B 426** (1998) 393.

[9] G.M. de Divitiis, R. Petronzio and L. Silvestrini, Nucl. Phys. **B 504** (1997) 45.

[10] D. Atwood, L. Reina and A. Soni, Phys. Rev. **D 53** (1996) 1199.

[11] T. Han, R.D. Peccei and X. Zhang, Nucl. Phys. **B 454** (1995) 527.

[12] R.D. Peccei and X. Zhang, Nucl. Phys. **B 337** (1990) 269.

[13] CDF Collaboration, *Search for flavor changing neutral current decay of the top quark in $p\bar{p}$ collisions at $\sqrt{s}$=1.8 TeV* Phys. Rev. Lett. **80** (1998) 2525.

[14] L.J. Reinders *et al.*, Physics Reports **127**, (1985) 1.

[15] ALEPH Collaboration, *ALEPH: A detector for electron-positron annihilation at LEP*, Nucl. Instrum. and Methods **A 294** (1990) 121.

[16] ALEPH Collaboration, *Performance of the ALEPH detector at LEP*, Nucl. Instrum. and Methods **A 360** (1995) 481.

[17] J.-F. Grivaz and F. Le Diberder, *Complementary analyses and acceptance optimization in new particle searches*, LAL-92-37;
ALEPH Collaboration, *Search for the standard model Higgs boson*, Phys. Lett. **B 313** (1993) 299.

[18] T. Sjöstrand, Comput. Phys. Commun. **82** (1994) 74.

[19] V. Khoze and T. Sjöstrand, Phys. Lett. **B 328** (1994) 466.

[20] F.A.Berends and R.Kleiss, Nucl. Phys. **B 178** (1981) 141.

[21] S. Jadach, B.F.L. Ward and Z. Wąs, Comput. Phys. Commun. **79** (1994) 503.

[22] S. Jadach, W. Placzek, M. Skrzypek, B.F.L. Ward and Z. Wąs, Comput. Phys. Commun. **119** (1999) 272.

[23] ALEPH Collaboration, *A precise measurement of* $\Gamma_Z \to b\bar{b}/\Gamma_Z \to$ hadrons, Phys. Lett. **B 313** (1993) 535.

[24] ALEPH Collaboration, *Measurement of the W Mass and Width in e^+e^- Collisions at 189 GeV*, CERN EP/2000-045, submitted to Eur. Phys. J. C.

[25] ALEPH Collaboration, *Search for the neutral Higgs bosons of the Standard Model and the MSSM in e^+e^- Collisions at $\sqrt{s}$ = 189 GeV*, CERN EP/2000-019, submitted to Eur. Phys. J. C.